npj | quantum materials

Perspective

Published in partnership with Nanjing University

https://doi.org/10.1038/s41535-025-00756-5

Altermagnetism classification

Check for updates

Sang-Wook Cheong ✉ & Fei-Ting Huang

Altermagnets are magnetic states with fully compensated spins and broken **PT** (**PT**: parity times time reversal) symmetry (i.e., spin-split bands). We classify three kinds of altermagnets in terms of broken **P** and **T**. Furthermore, strong altermagnets have spin-split bands without spin-orbit coupling (SOC), and weak altermagnets has spin-split bands only with non-zero SOC. These strong vs. weak altermagnets can be identified from the total number of symmetric spin rotation operations.

Altermagnetism[1–7] has been introduced as (almost) antiferromagnetism having time-reversal symmetry breaking by combining 'centrosymmetric crystallographic structure with local binary structural alternation' and 'collinear antiferromagnetism with time reversal and spatial inversion symmetries', even when translation is freely allowed. These altermagnets have broken **PT** (**P**: parity, **T**: time reversal, **PT**: parity times time reversal)[8] symmetry and spin-split bands[1,2], even in the non-relativistic limit, i.e., for zero spin-orbit coupling (SOC). The concept of altermagnetism has been extended to non-collinear (almost) antiferromagnets with multiple local structural variants and spin orientations[8–11]. These altermagnets with spin-split bands exhibit numerous spin-relevant phenomena such as various-order anomalous Hall effects[12–14], piezomagnetism[8,9,15,16], kinetomagnetism (i.e., current-induced magnetization)[17], etc. In this work, we broaden the definition of altermagnetism by focusing on the existence of spin-split bands rather than just structural alterations. We also include altermagnets that break spatial inversion symmetry while preserving time-reversal symmetry. The influence of spin-orbital coupling is categorized into weak (relativistic) and strong (non-relativistic) altermagnets. All strong collinear altermagnets discussed in the original proposal[3,5] in the literature are a subset of our M-type and S-type strong altermagnets. Our refined definition of altermagnetism is: magnetism with 'broken **PT** symmetry' and 'the ground state with full spin compensation in the non-relativistic limit'. This refined definition encompasses all instances of the original concept of altermagnetism, including those with collinear spins and alternating structural variations. Furthermore, we clarify the concept of 'almost' antiferromagnetism, introduce a classification scheme for three types of altermagnets (M-, S-, and A-types), and differentiate between strong and weak altermagnets through the consideration of straightforward spin rotation symmetry, utilizing the fundamental concept of the spin space/point group[18–20].

Sam Altermagnetism Classification

Figure 1a illustrates **PT** symmetry[21] operation, where a '+***k*** with spin up' state is linked to a '+***k*** with spin down' state. This means that the requirement for a system to have a spin-split bands is broken **PT** symmetry. We first define 'altermagnets as magnetic states with fully compensated spin angular momenta (spins) in the ground state and broken **PT** symmetry'. We focus on physical properties that are invariant to any translation, so we will always allow free translations. In other words, we always consider symmetry operations with a combination of any translation. For example, we will argue that the simple collinear antiferromagnetic state in Fig. 1c has unbroken **T** symmetry, while the ferromagnetic state is Fig. 1b still has broken **T** symmetry. There are two ways to have broken **PT** symmetry: [A] broken **T** symmetry and [B] unbroken **T** symmetry but broken **P** symmetry. Since we are discussing broken **PT** symmetry, we exclude the case of 'broken **T** symmetry, broken **P** symmetry and unbroken **PT** symmetry'. Also note that both 'broken **T**, unbroken **P** and broken **PT**', and 'broken **T**, broken **P** and broken **PT**' are parts of [A]. It turns out that Magnetization (***M***) along x has broken {**PT**,**T**,m_y,m_z,C_{2y},C_{2z},C_{3y},C_{3z}} with free rotation along x[22]. All magnetic point groups (MPGs), belonging the ferromagnetic point group, do have same or lower symmetry than ***M***, and are a subset of [A]. In our discussion, spin, spin angular momentum, and spin (magnetic) moment are interchangeable, similarly orbital angular momentum and orbital (magnetic) moment are all interchangeable, and magnetic moment means the total magnetic moment combining spin and orbital moments.

Thus, we have well-defined three types of altermagnets with fully compensated spin angular momenta (spins) and broken **PT** symmetry: [1] M-type: Broken **T** symmetry and belonging to the ferromagnetic point group, exhibiting SOC-induced spin splitting at the Γ point. There exists orbital ferrimagnetism, and uncompensated 'M'agnetization in the ground state. M-type is classified as type-I in our previous report[8]. [2] S-type: Broken **T**, no net magnetization, and 'S'ymmetric spin splitting, resulting in transverse piezomagnetism. S-type is classified as part of type-II in our previous report[8]. [3] A-type: Broken **P**, unbroken **T**, no net magnetization, and 'A'ntisymmetric spin splitting, resulting in no transverse piezomagnetism, but potentially having quadratic (even-order) AHE. Many A-type altermagnets are candidates for E-switchable altermagntism, featuring unbroken **T** symmetry, but broken **P** symmetry. S/A-type: Broken **P**, broken **T**, no net magnetization, and both 'S'ymmetric and 'A'ntisymmetric spin splitting. S/A-type altermagnets exhibit the properties of S-type altermagnets as well as those of A-type altermagnets. The advantage of SAM altermagnetism classification lies in its connection to various kinetomagnetism[17], which are based on broken **PT** symmetry. For instance, electric current can induce magnetization in various order (linear, high-odd

Keck Center for Quantum Magnetism and Department of Physics and Astronomy, Rutgers University, Piscataway, NJ, 08854, USA.
✉e-mail: sangc@physics.rutgers.edu

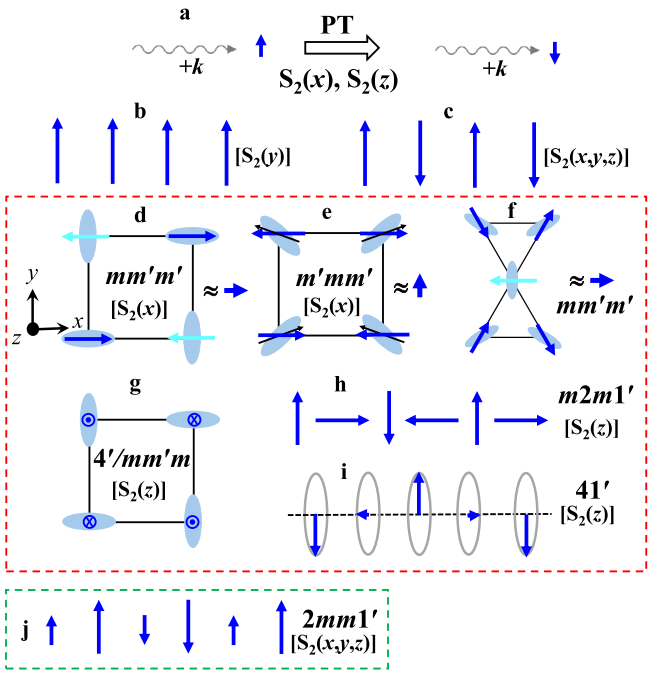

Fig. 1 | Various spin configurations. a PT, $\mathbf{S}_2(x)$, or $\mathbf{S}_2(z)$ symmetry operations link between 'electron crystal momentum $+k$ with up spin' and '$+k$ with down spin'. **b** Ferromagnetic spins. **c** antiferromagnetic spins. **b**, **c** are not altermagnets. **d** In-plane collinear spins with alternating local structures on square lattice. **e** In-plane collinear spins with alternating local structures on square lattice. **f** An alternating arrangement of three distinct crystallographic-director orientations and three spin orientations, which can be realized in Kagome lattice (see Fig. 3b). **g** Out-of-plane collinear spins with alternating local structures on square lattice. Blue arrows are spins, black arrows indicate canted magnetic moments due to the DM interaction, and dark/light blue arrows depict different orbital moments due to different g-tensor anisotropies. **h** Cycloidal spins. **i** Helical spins. **j** Up-up-down-down collinear two kinds of spins. $[\mathbf{S}_n(x,y,z)]$ indicates the presence of all of $\mathbf{S}_n(x)$, $\mathbf{S}_n(y)$, and $\mathbf{S}_n(z)$, meaning no spin-split bands occur for zero SOC, i.e., weak altermagnetism (green-dashed-box). $[\mathbf{S}_n(x)]$ means that only the $\mathbf{S}_n(x)$ symmetry is present, allowing for spin-split bands with $\boldsymbol{\sigma}(x)$ even for zero SOC, i.e. strong altermagnetism (red-dashed-box). M-type altermagnet: (**d**–**f**); S-type altermagnet: (**g**); and A-type altermagnets: (**h**–**j**).

order, or even order)[23], and this induced magnetization can be associated with various anomalous Hall effect (AHE) or piezomagnetism[9,12,15,16,24] as discussed in the following sections.

M-type and S-type altermagnets

M-type altermagnets exhibit full spin compensation, leading to their ferromagnetic behavior primarily governed by orbital angular momenta, which originates from SOC. Thus, the meaning of 'almost' antiferromagnetism mentioned in the introduction is associated with these possible net magnetizations or magnetic moments due to orbital angular momenta in M-type altermagnets when SOC is considered. An intriguing example of an M-type altermagnet, exhibiting orbital ferrimagnetism, is $CoMnO_3$[25,26], where Co^{2+} and Mn^{4+} have the same spins, but the opposite sign of SOC. When non-zero orbital angular momenta develop through SOC, then the full spin compensation can become partially broken, and spins can also result in non-zero net values through SOC, which is a supplementary effect. Emphasize that the symmetry of M-type altermagnets does not warrantee zero net spin moment. Rather than that, even if their spin configurations with broken **PT** symmetry have zero net spin moment (e.g., collinear antiferromagnetic spins), their net magnetization can be non-zero.

Three examples of M-type altermagnets with broken **T** and **PT** symmetry are shown in Fig. 1d–f. Figure 1e corresponds to the magnetic structure of NiF_2[27,28], while Fig. 1f illustrates the basic unit of Mn_3Sn[27,29]. All spins in Fig. 1d–f are fully compensated, at least, for zero SOC. The magnetic state in Fig. 1d can have a non-zero net orbital moment along x due to g-tensor anisotropy, and that in Fig. 1e can have a canted magnetic moment along y through the Dzyaloshinskii-Moriya (DM) interaction – this canted moment is mostly an orbital moment, but spins can also contribute through SOC. Figure 1g displays an example of S-type altermagnets with broken **T** and **PT** symmetry, representing the magnetic structure of CoF_2 or MnF_2[30,31]. Three-dimensional magnetic structures of NiF_2 and CoF_2 are illustrated in the Supplementary Note 1.

M-type altermagnets (Fig. 1d–f) with broken **T** and **PT** and non-zero magnetization, can exhibit linear AHE. S-type altermagnets with broken **T** and **PT** and zero magnetization can have transverse even-order current-induced magnetization (i.e., high-odd-order AHE). Thus, both M-type and S-type altermagnets can have transverse piezomagnetism. It has been reported that magnetic orthorhombic perovskites can exhibit M-type and S-type altermagnets[6]. The S-type altermagnet with ***4′/mm′m*** in Fig. 1g can exhibit transverse even-order current-induced magnetization along z with current along x or y (i.e., high-odd-order AHE with current along x (y) and Hall voltage along y (x)). Thus, it also shows transverse piezomagnetism with strain along x or y and induced magnetization along z.

A-type altermagnets

The cycloidal spin state in Fig. 1h accompanies electric polarization along y and the up-up-down-down spin state with two types of spins in Fig. 1j is associated with electric polarization along x[32]. Helical spins in Fig. 1i have chirality, i.e., broken all mirror symmetries. All of Fig. 1h–j with fully compensated spins have unbroken **T** and broken **P**, so belong to A-type altermagnets. A-type altermagnets with broken **P** and **PT** can exhibit transverse odd-order current-induced magnetization (i.e., even-order AHE), and some M-type and all S/A-type altermagnets do have broken all of **P, T** and **PT**, so they can also show transverse even-order as well as odd-order current-induced magnetization (i.e., odd-order as well as even-order AHE). For instance, the A-type altermagnet with a spiral spin structure in MPG ***m2m1′*** in Fig. 1h can show transverse odd-order current-induced magnetization along z (x) with current along x (z) (i.e., even-order AHE with current along x or z and Hall voltage along y).

The chiral A-type altermagnet with ***41′*** in Fig. 1i can show longitudinal current-induced magnetization along any direction. Cycloidal-spin-order-driven multiferroicity seen in materials like orthorhombic $TbMnO_3$[33] and $LiCu_2O_2$[34], as well as pyroelectric $Ni_2Mo_3O_8$[35,36] show similar spin structures. The A-type altermagnet with ***2mm1′*** in Fig. 1j can show transverse odd-order current-induced magnetization along z (y) with current along y (z) (i.e., even-order AHE with current along y or z and Hall voltage along x). Materials such as MnS_2[37], $HoMnO_3$[38] show similar spin structures. Note that incommensurate (cycloidal/helical) spin modulations, including odd-period spin modulations, usually accompany antiphase domains, i.e., domains with phase shifts. When all antiphase domains are considered, those spin modulations always have unbroken **T** symmetry, just like commensurate even-period spin modulations.

Magnetic point group analysis

90 out of 122 MPGs have broken **PT**[39,40], and 31 out of these 90 MPGs belong to the ferromagnetic point group and do have broken **T** symmetry. When any of these 31 MPGs have fully compensated spins, then they belong to M-type altermagnets. 38 out of these 90 MPGs do not belong to the ferromagnetic point group but do have broken **T** symmetry. All these 38 MPGs belong to S-type altermagnets, since all of them do have fully compensated spins. There are 21 MPGs with unbroken **T**, broken **P**, and broken **PT** symmetry and all these 21 MPGs belong to A-type altermagnet, since all of them do have fully compensated spins. Among 38 S-type altermagnets, 27 can have broken **P, T** and **PT**, i.e., S/A type-altermagnets. These classifications are summarized in Fig. 2.

Figure 2 represents an expanded diagram compared to the one in our previous report[8]. The updated analysis differs from our earlier work due to a revised approach that now includes all directions, rather than focusing on

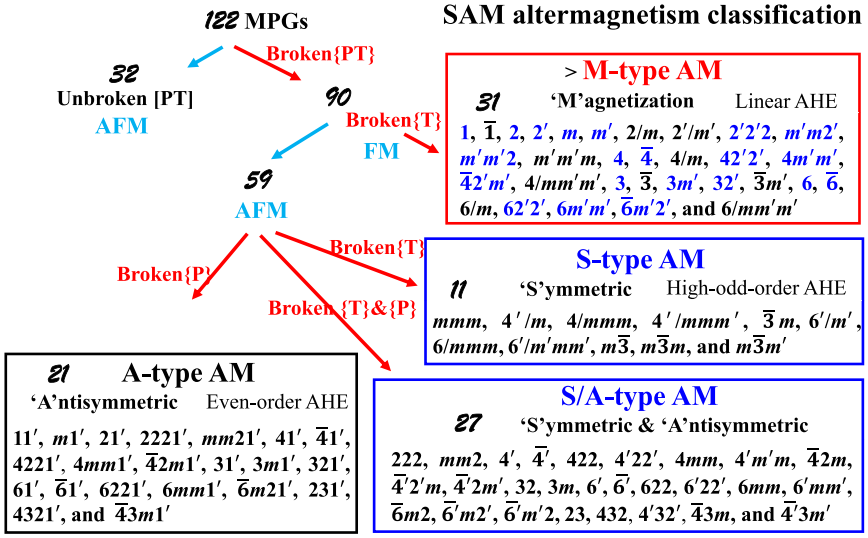

Fig. 2 | MPG classification for M-type, S-type, and A-type altermagnets. 31 MPGs belonging to the ferromagnetic point group can be M-type AM if they have fully compensated spins, there are 11 MPGs for S-type AM, 27 MPGs for S/A-type, and there exist 21 MPGs for A-type AM. Square brackets [] denote unbroken symmetry, while curly brackets {} represent broken symmetry. All altermagnets have broken **PT**, M-type and S-type AM have broken **T**, S/A-type has broken **T** and **P**. A-type altermagnets have unbroken **T** and broken **P**. MPGs in blue and S/A-type AM have broken all of **P, T**, and **PT**. M-type altermagnets show non-zero net magnetization (i.e., linear AHE), S-type altermagnets can have transverse even-order current-induced magnetization (i.e., high-odd-order AHE), and A-type altermagnets can exhibit transverse odd-order current-induced magnetization (i.e., even-order AHE). Thus, both M-type and S-type altermagnets can have transverse piezomagnetism. MPGs in blue for M-type and the S/A-type altermagnets can also show transverse odd-order current-induced magnetization (i.e., even-order AHE).

the principal axes (high-symmetry axes) aligned with the basis vectors of conventional crystallographic coordinate systems[41]. For example, in our previous report, the MPG analysis was restricted to symmetries along the *x*, *y*, and *z* directions for orthorhombic MPGs. The current analysis, however, incorporates symmetries for allowed properties of altermagnets along all directions. This refined classification provides a more inclusive and systematic consideration of symmetries and physical properties along various directions. Both approaches are useful in different manners – in terms of simplicity, the approach in this paper may be better, but in terms of performing experiments, that in ref. 8 can be useful, since experiments tend to be performed along symmetric directions, and the magnitudes of the relevant effects tend to be large along symmetric directions.

P-wave magnetism is a subset of A-type altermagnetism in our classification. It was proposed for CeNiAsO with non-collinear spins and the MPG of **21**′[27,42,43]. In A-type altermagnets, spin splitting in A-type altermagnets is antisymmetric with respect to *k* due to broken **P** symmetry. This splitting can occur without SOC and arises through 'magnetic order'. While this *k*-antisymmetric spin splitting in A-type altermagnets is sometime Rashba-type, it is not always the case (see Supplementary Note 2). Additional examples of ***mmm*** (S-type, MnTe)[15,44,45], ***6′mm′*** (S/A-type, $Fe_2Mo_3O_8$)[46], and ***6 m′m′*** (M-type, $Mn_2Mo_3O_8$)[47] are discussed for their physical properties in the Supplementary Note 1. The MPGs ***6′mm′*** and ***6 m′m′*** are particularly interesting due to broken all of **P, T**, and **PT** symmetries, leading to a variety of physical properties and phenomena.

Spin Rotation Operation

Broken **PT** symmetry alone doesn't allow us to determine whether the spin spitting of bands is due to SOC, which is a relativistic effect, or if it can still exist in the non-relativistic limit (i.e. for zero SOC). We now introduce a Spin Rotation Operation $\mathbf{S_n}(r)$ around the *r* axis, which rotates all spins at their own locations by $2\pi/n$ without rotating the crystallographic structure. When SOC is turned off, this $\mathbf{S_n}(r)$ does not cost any energy, but this $\mathbf{S_n}(r)$ symmetry may or may not exist in a given magnetic state along a given axis. Note that the presence of this $\mathbf{S_n}(r)$ symmetry can vary even among magnetic states with the identical magnetic point group. This $\mathbf{S_n}(r)$ in real space accompanies $\boldsymbol{\sigma}(r)$ (spin expectation value along *r* in crystal momentum space) without changing *k*.

In Fig. 1a, $\mathbf{S_2}(x)$ and $\mathbf{S_2}(z)$ link '$+\boldsymbol{k}$ with spin up' and '$+\boldsymbol{k}$ with spin down'. This means that the requirement for a system to have a spin-split bands for zero SOC is, at most, one unbroken $S_n(r)$ in addition to broken **PT** symmetry. Having more than one axis for $S_n(r)$ invariance prevents strong altermagnetism, making the absence of such symmetry a necessary condition for the emergence of strong altermagnetism. For zero SOC, a system with unbroken $\mathbf{S_2}(y)$ symmetry, as shown in Fig. 1b, cannot have $\boldsymbol{\sigma}(x)$ and $\boldsymbol{\sigma}(z)$, but may have $\boldsymbol{\sigma}(y)$, meaning spin-up and spin-down splitting along the *y*-axis. The spin-split band and symmetry are demonstrated in Supplementary Note 2. The procedures of considering spin rotation operations for exemplary magnetic states are illustrated in the Supplementary Note 3.

Strong v.s. Weak Altermagnets

With the concept of spin rotation operation, now, we can distinguish strong vs. weak altermagnetism: strong altermagnets do have spin-split bands through exchange coupling in the non-relativistic limit, i.e. for zero SOC, and weak altermagnets can have spin-split bands only with non-zero SOC. Note that the definition of strong and weak altermagnetism defined here differ from those in a recent report[48]. For orthogonal *x*, *y* and *z* axes, a magnetic system 'cannot' have spin-split bands for zero SOC if it has two or more spin rotation symmetries out of $\mathbf{S_n}(x)$, $\mathbf{S_n}(y)$, and $\mathbf{S_n}(z)$, since it accompanies the presence of two or more spin rotation symmetries out of $\boldsymbol{\sigma}(x)$, $\boldsymbol{\sigma}(y)$, and $\boldsymbol{\sigma}(z)$ in *k* space[20]. The orthogonal *x*, *y* and *z* axes are along any directions, not just along crystallographic symmetric directions. For example, the ferromagnetic state in Fig. 1b has only $\mathbf{S_n}(y)$, so it can have spin-split bands with $\boldsymbol{\sigma}(y)$ for zero SOC, but the antiferromagnetic state in Fig. 1c has all of $\mathbf{S_n}(x)$, $\mathbf{S_n}(y)$, and $\mathbf{S_n}(z)$ symmetries, so cannot have spin-split bands for zero SOC.

M-type altermagnet in Figs. 1d, e, and S-type altermagnet in Fig. 1g have $\mathbf{S_2}(x)$, $\mathbf{S_2}(x)$, and $\mathbf{S_2}(z)$ symmetries, respectively, so they can have spin-split bands through exchange coupling with $\boldsymbol{\sigma}(x)$, $\boldsymbol{\sigma}(x)$, and $\boldsymbol{\sigma}(z)$, respectively, for zero SOC. M-type altermagnet in Fig. 1f has no $\mathbf{S_n}(x,y,z)$ symmetry, so can have spin-split bands with any of $\boldsymbol{\sigma}(x)$, $\boldsymbol{\sigma}(y)$, and $\boldsymbol{\sigma}(z)$ for zero SOC. Thus, all of Fig. 1d–g with broken **T** symmetry are strong altermagnets. It turns out that A-type altermagnets in Fig. 1h, i have $\mathbf{S_2}(z)$ symmetry, so can have spin-split bands with $\boldsymbol{\sigma}(z)$ for zero SOC. However, A-type altermagnet in Fig. 1j has all of $\mathbf{S_2}(x)$, $\mathbf{S_2}(y)$, and $\mathbf{S_2}(z)$, so cannot have spin-split bands for zero SOC. Thus, A-type altermagnets in Fig. 1h, i are strong altermagnets and A-type altermagnet in Fig. 1j is a weak altermagnet. Since electric polarizations are associated with both the strong altermagnet in Fig. 1h and the weak altermagnet in Fig. 1j, their altermagnetic spin-split bands can be switched by external electrics fields.

The procedures of considering spin rotation operations for exemplary magnetic states are illustrated in the Supplementary Note 3. We emphasize that the spin structures in Fig. 1h, j have basically the same MPG, but that in

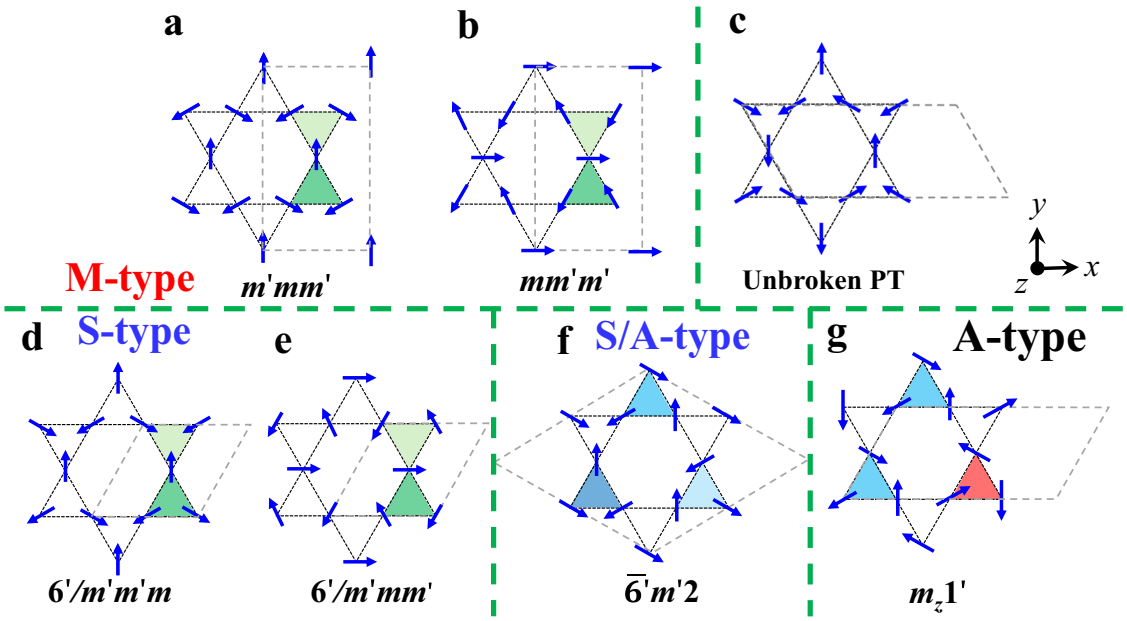

Fig. 3 | Various spin configuration on Kagome lattices. a, **b** M-type altermagnets. **c** A spin configuration with unbroken **PT**. **d**–**f** S-type altermagnets. **g**, A-type altermagnet. All configurations except **c** have broken **PT**. (**a**, **b**, **d**, **e**) have broken **T** and unbroken **P**. Green and light green units indicate inversion relation. **f** has broken all of **P, T** and **PT** with blue units representing a three-fold relationship. (**g**) has unbroken **T** and broken **P**, with blue and red units representing time-reversal relation. Grey dashed lines outline the magnetic unit cells.

Fig. 1h is a strong altermagnet, and that in Fig. 1j is a weak altermagnet, which clearly demonstrates that MPG itself as discussed in our previous work[8] is not sufficient to identify strong vs. weak altermagnets. All strong collinear altermagnets discussed in the original proposal[3,5] in the literature are a subset of our M-type and S-type strong altermagnets. M-type strong altermagnets can exhibit spin-split bands without SOC but acquire net orbital moments when SOC is present. A-type strong altermagnets can display spin-split bands without SOC while maintaining time-reversal invariance.

In the cases of M-type and S-type altermagnets with broken **T** symmetry and "collinear" spins, we can prove that they are always strong altermagnets. When the collinear spins are along z, $\mathbf{S}_2(x)$ and $\mathbf{S}_2(y)$ are identical with **T** symmetry operation, so they are broken, even though $\mathbf{S}(z)$ is unbroken. Thus, they are strong altermagnets and can have spin-split bands with $\boldsymbol{\sigma}(z)$ for zero SOC. Likely, the same argument works even for M-type and S-type altermagnets with broken **T** symmetry and non-collinear spins, but the exact proof seems depending on the magnetic unit cell. Now, we can prove that all 'collinear' A-type altermagnets with unbroken **T** symmetry and broken **P** symmetry such as the polar magnetic state in Fig. 1j are always weak. When the collinear spins are along z, $\mathbf{S}_2(x)$ and $\mathbf{S}_2(y)$ are identical with **T** symmetry operation, so they are unbroken, in addition to unbroken $\mathbf{S}(z)$. Thus, they are always weak. However, some 'non-collinear' A-type altermagnets with unbroken **T** symmetry and broken **P** symmetry such as the polar magnetic state in Fig. 1h and the chiral magnetic state in Fig. 1i are strong, as discussed earlier.

Strong Noncollinear Altermagnets on Kagome Lattice

Kagome lattice turns out to be a wonderful system where all three types of altermagnetism can be realized. All of Fig. 3 have fully compensated spins on Kagome lattice. Figure 3c has unbroken **PT** while the rest of Fig. 3 do have broken **PT**. Figure 3a, b have broken **T**, and do have net magnetic moments (along y, and x, respectively). Figure 3d–f have broken **T**, and do not have net magnetic moments. Figure 3f has broken all of **P, T** and **PT**, and Fig. 3g has unbroken **T** and broken **P**. Thus, Fig. 3a, b, d–g are examples of M-type, S-type, S/A-type and A-type altermagnets on Kagome lattice, respectively. Figure 3a with $\boldsymbol{m'mm'}$ can have a net magnetic moment along y and is realized in $Mn_3Ge(Ga)$[49,50], and Fig. 3b with $\boldsymbol{mm'm'}$ can have a net magnetic moment along x and is realized in Mn_3Sn[16,29,51]. All of these M-type altermagnets can exhibit linear anomalous Hall effects in the planes perpendicular to the net magnetic moment directions. S-type altermagnet on Kagome lattice shown in Fig. 3d with $\boldsymbol{6'/m'm'm}$, which can happen in each (111) layer of cubic $Mn_3Ir(Pt,Rh)$[52], exhibit transverse even-order current-induced magnetization with current along x and induced magnetization along y, high-odd-order AHE with current along x and Hall voltage along z, and transverse piezomagnetism with uniaxial stress along x and induced magnetization along y.

Figure 3f with $\boldsymbol{\bar{6}'m'2}$ can exhibit transverse even-order current-induced magnetization with current along x and induced magnetization along y, high-odd-order AHE with current along x and Hall voltage along z, and transverse piezomagnetism with uniaxial stress along x and induced magnetization along y. A-type altermagnet in Fig. 3g with $\boldsymbol{m1'}$ can have electric polarization in the xy plane. This A-type altermagnet can exhibit even-order AHE with applied current perpendicular to the electric polarization and Hall voltage along the electric polarization. All of these altermagnets on Kagome lattice in Fig. 3a, b, 3d–g have, at most, $\mathbf{S}_2(z)$ symmetry, so they are strong altermagnets and can have spin-split bands with, at least, $\boldsymbol{\sigma}(z)$ for zero SOC.

Conclusion

The definition of Altermagnets is refined: magnetism with 'broken **PT** symmetry' and 'the ground state with full spin compensation in the non-relativistic limit'. – here, collinearity or non-collinearity is not important. Three kinds of altermagnets are identified: M-type: broken **T** symmetry and nonzero net magnetic moments, S-type: broken **T** symmetry, and zero net magnetic moments, and A-type: unbroken **T** and broken **P** symmetries. S-type altermagnets do not belong to the ferromagnetic point group, and **P** may or may not be broken in S-type altermagnets. M-type altermagnets, belong to the ferromagnetic point group, show linear AHE, transverse even-order current induced magnetization, and transverse piezomagnetism. S-type altermagnets do exhibit high odd-order AHE, transverse even-order

current induced magnetization, and transverse piezomagnetism. A-type altermagnets allows quadratic AHE, transverse odd-order current induced magnetization, and transverse piezoelectricity. In fact, all altermagnets exhibit some form of kinetomagnetism, i.e. current-induced magnetization in various orders.

We also classified strong vs. weak altermagnets: strong altermagnets have spin-split bands through exchange coupling even for zero SOC, and weak altermagnets have spin-split bands only for non-zero SOC. The total number of symmetric orthogonal spin rotation operations determines if an altermagnet is strong or weak. All 'collinear' M-type and S-type altermagnets are strong altermagnets, and all 'collinear' A-type altermagnets are weak altermagnets. These clear and comprehensive classifications of altermagnets based on the **PT** symmetry approach provide a far-reaching perspective for future research on altermagnetism.

Data availability

All study data is included in the article.

Received: 15 September 2024; Accepted: 24 March 2025;
Published online: 12 April 2025

References

1. Yuan, L. D., Wang, Z., Luo, J. W., Rashba, E. I. & Zunger, A. Giant momentum-dependent spin splitting in centrosymmetric low-Z antiferromagnets. *Phys. Rev. B* **102**, 014412 (2020).
2. Hayami, S., Yanagi, Y. & Kusunose, H. Momentum-dependent spin splitting by collinear antiferromagnetic ordering. *J. Phys. Soc. Jpn.* **88**, 123702 (2019).
3. Šmejkal, L., Sinova, J. & Jungwirth, T. Beyond conventional ferromagnetism and antiferromagnetism: a phase with nonrelativistic spin and crystal rotation symmetry. *Phys. Rev. X* **12**, 031042 (2022).
4. Mazin, I. Editorial: Altermagnetism - a new punch line of fundamental magnetism. *Phys. Rev. X* **12**, 040002 (2022).
5. Šmejkal, L., Sinova, J. & Jungwirth, T. Emerging research landscape of altermagnetism. *Phys. Rev. X* **12**, 040501 (2022).
6. Fernandes, R. M., De Carvalho, V. S., Birol, T. & Pereira, R. G. Topological transition from nodal to nodeless Zeeman splitting in altermagnets. *Phy. Rev. B* **109**, 024404 (2024).
7. Bhowal, S. & Spaldin, N. A. Ferroically ordered magnetic octupoles in d-wave altermagnets. *Phys. Rev. X* **14**, 011019 (2024).
8. Cheong, S. -W. & Huang, F. -T. Altermagnetism with non-collinear spins. *npj quantum Mater.* **9**, 13 (2024).
9. Radaelli, P. G. A. tensorial approach to 'altermagnetism'. *Phys. Rev. B* **110**, 214428 (2024).
10. Hayami, S., Yanagi, Y. & Kusunose, H. Spontaneous antisymmetric spin splitting in noncollinear antiferromagnets without spin-orbit coupling. *Phys. Rev. B* **101**, 220403 (2020).
11. Zhu, Y. P. et al. Observation of plaid-like spin splitting in a noncoplanar antiferromagnet. *Nature* **626**, 523–528 (2024).
12. Cheong, S. -W. & Huang, F. -T. Emergent phenomena with broken parity-time symmetry: Odd-order versus even-order effects. *Phys. Rev. B* **109**, 104413 (2024).
13. Nagaosa, N., Sinova, J., Onoda, S., MacDonald, A. H. & Ong, N. P. Anomalous Hall effect. *Rev. Mod. Phys.* **82**, 1539–1592 (2009).
14. Šmejkal, L. et al. Crystal time-reversal symmetry breaking and spontaneous Hall effect in collinear antiferromagnets. *Sci. Adv.* **6**, eaaz8809 (2020).
15. Aoyama, T. & Ohgushi, K. Piezomagnetic properties in altermagnetic MnTe. *Phys. Rev. Mater.* **8**, L041402 (2024).
16. Ikhlas, M. et al. Piezomagnetic switching of the anomalous Hall effect in an antiferromagnet at room temperature. *Nat. Phys.* **18**, 1086–1093 (2022).
17. Cheong, S. -W. & Huang, F. -T. Kinetomagnetism of chirality and its applications. *Appl. Phys. Lett.* **125**, 060501 (2024).
18. Litvin, D. B. Spin point groups. *Acta cryst. A* **33**, 279–287 (1977).
19. Liu, P., Li, J., Han, J., Wan, X. & Liu, Q. Spin-group symmetry in magnetic materials with negligible spin-orbit coupling. *Phys. Rev. X* **12**, 021016 (2022).
20. Brinkman, W. F. & Elliott, R. J. Theory of spin-space groups. *Proc. R. Soc. Lond. A* **294**, 343–358 (1966).
21. Özdemir, ŞK., Rotter, S., Nori, F. & Yang, L. Parity–time symmetry and exceptional points in photonics. *Nat. Mater.* **18**, 783–798 (2019).
22. Cheong, S. -W. & Huang, F. -T. Trompe L'oeil Ferromagnetism—magnetic point group analysis. *npj Quantum Mater.* **8**, 73 (2023).
23. Yoda, T., Yokoyama, T. & Murakami, S. Current-induced orbital and spin magnetizations in crystals with helical structure. *Sci. Rep.* **5**, 12024 (2015).
24. Ma, H. Y. et al. Multifunctional antiferromagnetic materials with giant piezomagnetism and noncollinear spin current. *Nat. Commun.* **12**, 2846 (2021).
25. Bozorth, R. M. & Walsh, D. E. Ferromagnetic moment of $CoMnO_3$. *J. Phys. Chem. Sol.* **5**, 299–301 (1958).
26. Koizumi, H., Inoue, J. I. & Yanagihara, H. Magnetic anisotropy and orbital angular momentum in the orbital ferrimagnet $CoMnO_3$. *Phy. Rev. B* **100**, 224425 (2019).
27. Gallego, S. V. et al. MAGNDATA: towards a database of magnetic structures. I. The commensurate case. *J. Appl. Crystallogr.* **49**, 1750–1776 (2016).
28. Brown, P. J. & Forsyth, J. B. A neutron diffraction study of weak ferromagnetism in nickel fluoride. *J. Phys. C.* **14**, 5171–5184 (1981).
29. Nakatsuji, S., Kiyohara, N. & Higo, T. Large anomalous Hall effect in a non-collinear antiferromagnet at room temperature. *Nature* **527**, 212–215 (2015).
30. Moriya, T. Piezomagnetism in CoF_2. *J. Phys. Chem. Solids* **11**, 73–77 (1959).
31. Jauch, W., Reehuis, M. & Schultz, A. J. γ-ray and neutron diffraction studies of CoF_2: magnetostriction, electron density and magnetic moments. *Acta cryst. A* **60**, 51–57 (2004).
32. Cheong, S. -W. & Mostovoy, M. Multiferroics: a magnetic twist for ferroelectricity. *Nat. Mater.* **6**, 13–20 (2007).
33. Kenzelmann, M. et al. Magnetic inversion symmetry breaking and ferroelectricity in $TbMnO_3$. *Phy. Rev. Lett.* **95**, 087206 (2005).
34. Park, S., Choi, Y. J., Zhang, C. L. & Cheong, S. W. Ferroelectricity in an S=1/2 chain cuprate. *Phy. Rev. Lett.* **98**, 057601 (2007).
35. Tang, Y. S. et al. Metamagnetic transitions and magnetoelectricity in the spin-1 honeycomb antiferromagnet $Ni_2Mo_3O_8$. *Phys. Rev., B* **103**, 014112 (2021).
36. Yadav, P. et al. Noncollinear magnetic order, in-plane anisotropy, and magnetoelectric coupling in a pyroelectric honeycomb antiferromagnet $Ni_2Mo_3O_8$. *Phy. Rev. Res.* **5**, 033099 (2024).
37. Hastings, J. M., Elliott, N. & Corliss, L. M. Antiferromagnetic structures of MnS_2, $MnSe_2$, and $MnTe_2$. *Phys. Rev.* **115**, 13–17 (1959).
38. Muñoz, A. et al. Complex magnetism and magnetic structures of the metastable $HoMnO_3$ perovskite. *Inorg. Chem.* **40**, 1020 (2001).
39. Yatsushiro, M., Kusunose, H. & Hayami, S. Multipole classification in 122 magnetic point groups for unified understanding of multiferroic responses and transport phenomena. *Phys. Rev. B* **104**, 054412 (2021).
40. Yuan, L. D., Wang, Z., Luo, J. W. & Zunger, A. Prediction of low-Z collinear and noncollinear antiferromagnetic compounds having momentum-dependent spin splitting even without spin-orbit coupling. *Phys. Rev. Mater.* **5**, 014409 (2021).
41. Hahn, T. International tables for crystallography. Volume A, Space-group symmetry, (International Union of Crystallography by Kluwer Academic Publishers, Dordrecht, 1996).
42. Wu, S. et al. Incommensurate magnetism near quantum criticality in CeNiAsO. *Phys. Rev. Lett.* **122**, 197203 (2019).
43. Anna Birk, H. et al. P-wave magnets. *arXiv:2309.01607* (2024).
44. Mazin, I. I. Altermagnetism in MnTe: Origin, predicted manifestations, and routes to detwinning. *Phys. Rev. B* **107**, L100418 (2023).

45. Kunitomi, N., Hamaguchi, Y. & Anzai, S. Neutron diffraction study on manganese telluride. *J. Phys. Colloq.* **25**, 568–574 (1964).
46. Wang, Y. et al. Unveiling hidden ferrimagnetism and giant magnetoelectricity in polar magnet $Fe_2Mo_3O_8$. *Sci. Rep.* **5**, 12268 (2015).
47. Kurumaji, T., Ishiwata, S. & Tokura, Y. Diagonal magnetoelectric susceptibility and effect of Fe-doping in a polar ferrimagnet $Mn_2Mo_3O_8$. *Phys. Rev. B* **95**, 045142 (2016).
48. Krempaský, J. et al. Altermagnetic lifting of Kramers spin degeneracy. *Nature* **626**, 517–522 (2023).
49. Nayak, A. K. et al. Large anomalous Hall effect driven by a nonvanishing Berry curvature in the noncolinear antiferromagnet Mn_3Ge. *Sci. Adv.* **2**, e1501870 (2016).
50. Park, P. et al. Magnetic excitations in non-collinear antiferromagnetic Weyl semimetal Mn_3Sn. *npj Quantum Mater.* **3**, 63 (2018).
51. Liu, J. & Balents, L. Anomalous Hall effect and topological defects in antiferromagnetic Weyl semimetals: Mn_3Sn/Ge. *Phys. Rev. Lett.* **119**, 087202 (2017).
52. Chen, H., Niu, Q. & Macdonald, A. H. Anomalous hall effect arising from noncollinear antiferromagnetism. *Phys. Rev. Lett.* **112**, 017205 (2014).

Acknowledgements

This work was supported by the DOE under Grant No. DOE: DE-FG02-07ER46382.

Author contributions

S.W.C. conceived and supervised the project. F.-T.H. conducted magnetic point group analysis. S.W.C. wrote the remaining part.

Competing interests

Author S.-W. Cheong serves as editor-in-chief of this journal and had no role in the peer-review or decision to publish this manuscript.

Additional information

Supplementary information The online version contains supplementary material available at https://doi.org/10.1038/s41535-025-00756-5.

Correspondence and requests for materials should be addressed to Sang-Wook Cheong.

Reprints and permissions information is available at http://www.nature.com/reprints

Publisher's note Springer Nature remains neutral with regard to jurisdictional claims in published maps and institutional affiliations.

Open Access This article is licensed under a Creative Commons Attribution-NonCommercial-NoDerivatives 4.0 International License, which permits any non-commercial use, sharing, distribution and reproduction in any medium or format, as long as you give appropriate credit to the original author(s) and the source, provide a link to the Creative Commons licence, and indicate if you modified the licensed material. You do not have permission under this licence to share adapted material derived from this article or parts of it. The images or other third party material in this article are included in the article's Creative Commons licence, unless indicated otherwise in a credit line to the material. If material is not included in the article's Creative Commons licence and your intended use is not permitted by statutory regulation or exceeds the permitted use, you will need to obtain permission directly from the copyright holder. To view a copy of this licence, visit http://creativecommons.org/licenses/by-nc-nd/4.0/.

© The Author(s) 2025